Cancer Chemother Pharmacol (2009) 63:837–850
DOI 10.1007/s00280-008-0810-y

ORIGINAL ARTICLE

Role of RNase L in apoptosis induced by 1-(3-*C*-ethynyl-*β*-D-*ribo*-pentofuranosyl)cytosine

Tomoharu Naito · Tatsushi Yokogawa · Satoshi Takatori · Kazato Goda · Akiko Hiramoto · Akira Sato · Yukio Kitade · Takuma Sasaki · Akira Matsuda · Masakazu Fukushima · Yusuke Wataya · Hye-Sook Kim

Received: 30 April 2008 / Accepted: 18 July 2008 / Published online: 31 July 2008

Abstract
Purpose 1-(3-*C*-Ethynyl-*β*-D-*ribo*-pentofuranosyl)cytosine (ECyd), a ribonucleoside analog, has a potent cytotoxic activity against cancer cells. The present studies have been performed to elucidate the overall mechanisms of ECyd-induced apoptotic cell death.
Methods Cultured cells of mouse mammary carcinoma FM3A and human fibrosarcoma HT 1080 lines were used. The efficacy of RNA synthesis inhibition by ECyd was assessed by kinetic analysis using nuclei isolated from FM3A cells. RNA status in ECyd-treated cells was investigated by Northern blots, and the cleavage sites of RNA were identified by rapid amplification of 5′ cDNA ends (5′-RACE). The effect of protein functions on the ECyd-induced apoptotic pathway was analyzed by siRNA and immunohistochemical techniques. Apoptotic cells were detected by TdT-mediated dUTP-biotin Nick End Labeling (TUNEL) assay.
Results ECyd induces inhibition of RNA synthesis in vitro and in vivo, which appears to be a major cause for the apoptosis. It is known that ECyd is converted inside the cell into its 5′-triphosphate (ECTP). We have now found in test-tube experiments that ECTP strongly inhibits the activity of RNA polymerase I by competing with CTP. In the absence of robust RNA synthesis, the cellular RNAs would be destined to break down. RNase L was found to be playing a role in the breakdown: thus, the 28S rRNA-fragmentation pattern observed for the ECyd-treated cells was very similar to that observable in an in vitro treatment of the 28S ribosomes with RNase L. Association of RNase L with the cytotoxic action of ECyd was confirmed by use of the siRNA-mediated suppression of the cellular RNase L. Thus, the cells in which the RNase L was knocked-down were highly resistant to the cytotoxic action of ECyd. Further events, downstream of the RNase L action that can lead to the eventual apoptosis, would conceivably involve the phosphorylation of c-jun N-terminal kinase and subsequent decrease in mitochondrial membrane-potential. Evidence to support this flow of events was obtained by siRNA-experiments.
Conclusion The results from this study demonstrated that RNase L is activated after the inhibition of RNA polymerase, and induces mitochondria-dependent apoptotic pathway. We propose this new role for RNase L in the apoptotic mechanism. These findings may open up the possibility of finding new targets for anticancer agents.

Keywords ECyd · RNase L · JNK · Apoptosis · RNA synthesis · 28S rRNA fragmentation

Tomoharu Naito and Tatsushi Yokogawa have contributed equally to the main findings of the paper.

T. Naito · T. Yokogawa · S. Takatori · K. Goda · A. Hiramoto · A. Sato · M. Fukushima · Y. Wataya · H.-S. Kim (✉)
Faculty of Pharmaceutical Sciences,
Okayama University, 1-1-1 Tsushimanaka,
Okayama 700-8530, Japan
e-mail: hskim@cc.okayama-u.ac.jp

Y. Kitade
Department of Biomolecular Science,
Faculty of Engineering, Gifu University,
1-1 Yanagido, Gifu 501-1193, Japan

T. Sasaki
Cancer Research Institute, Kanazawa University,
13-1 Takara-machi, Kanazawa 920-0934, Japan

A. Matsuda
Graduate School of Pharmaceutical Sciences,
Hokkaido University, Kita-12 Nishi-6,
Kita-ku, Sapporo 060-0812, Japan

Introduction

Many anticancer agents are DNA synthesis-inhibitors, targeting at the rapidly proliferating tumor cells. However, their effects on solid tumors are often unsatisfactory. Between solid tumor- and normal-cells, the growth rates are not greatly different. In solid tumors, the proportion of cell number at the S phase is smaller than that of the rapidly proliferating tumor cells, and the cells in solid tumors are heterogeneous in the sense that individual cells activate various phases of cell cycle. For this reason, we considered the need for the inhibition of RNA synthesis, which occurs throughout the cell cycle except in the M phase, to potentiate the anticancer effect against solid tumors.

1-(3-*C*-Ethynyl-*β*-D-*ribo*-pentofuranosyl)cytosine (ECyd), a nucleoside analog originally designed as a possible inhibitor of cellular RNA synthesis, has been shown to exhibit strong activities against carcinogenesis [1, 2]. In our earlier experiments using cultured cells, we have shown that the metabolic conversion of ECyd into its active form, 5′-triphosphate (ECTP) takes place readily in cancer cells, but only very slowly in normal cells [3, 4]. It was noted that cellular RNA synthesis was indeed strongly inhibited, presumably by the presence of the CTP analog, ECTP, within the cell, and this inhibition appeared to trigger the apoptotic cell death. Although apoptosis-like cell death is induced in the ECyd-treated cells, it is still not clear what activates the apoptotic signal after the RNA synthesis inhibition. Identification of such factors may lead to devices for improving the antitumorigenic efficacy of ECyd. We have now performed extensive studies for elucidating the overall picture of the ECyd-induced death of cancer cells, mouse mammary carcinoma FM3A and human fibrosarcoma HT 1080. As described below, the flow of events leading to the apoptosis was largely revealed; a process in which RNase L plays an important role.

Materials and methods

Materials

ECyd was synthesized as described previously [2]. Actinomycin D and ara-C were purchased from Sigma-Aldrich (St Louis, MO, USA). [8-^{3}H]GTP and [γ-^{32}P]ATP were obtained from Amersham Biosciences (Piscataway, NJ, USA). Oligonucleotides used in Northern blot hybridization and in RACE (Rapid Amplification of 5′ cDNA Ends) were obtained from Sawady Technology (Tokyo, Japan). RNase T_1, RNase A, lipofectin and lipofectamine 2000 were purchased from Invitrogen (Carlsbad, CA, USA). Human recombinant RNase L was prepared as described previously [5]. The 2-5A used was p5′(A2′p5′)$_2$A synthesized as reported [6]. The antibody to c-jun NH_2-terminal kinase (JNK) was from Cell Signaling Technology (Beverly, MA, USA), that to *β*-actin was from Sigma-Aldrich, and that to GAPDH was from Trevigen (Gaithersburg, MD, USA). Preparation of monoclonal antibody to human RNase L and synthesis of siRNA were done as previously reported [7]. A pair of RNase L-siRNA (siRNL) and control siRNA (siMis) were prepared as reported [7]. The sequences of these siRNAs were as follows: active siRNAs (siRNL) 5′-GCUGUUCAAAACGAAGAUGTT-3′ 3′-TTCGACA AGUUUUGCUUCUAC-5′; control siRNAs (siMis) 5′-GC UAUUCUAAAGGAAUAUGTT-3′ 3′-TTCGAUAAGA UUUCCUUAUAC-5′. The TT dinucleotide attached to each of these oligonucleotides at their 3′ overhang was a deoxythymidine dimer with a carbamate linkage that enhances the siRNA silencing activities.

Cell culture and drug treatments

The cultivation of cells, mouse mammary tumor FM3A (F28-7, Japanese Cancer Research Resources Bank, Tokyo, Japan) and human fibrosarcoma HT 1080 (American Type Culture Collection, Rockville, MD, USA), was performed as previously reported [3, 4]. In several experiments, it was difficult to use FM3A because the cells are suspension-cultured cell lines lacking adhesive characters. In such cases, we used adhesive type cells HT 1080. Cell viability was estimated by the trypan blue exclusion method using a hemocytometer. The 50% growth-inhibitory concentration of ECyd against FM3A and HT 1080 cells is 3×10^{-8} M and 1.3×10^{-8} M, respectively. For each cell line, drug treatments were performed at doses 100-fold, the 50% growth-inhibitory concentration.

Transfection

Transfections of 2-5A and siRNAs were done using lipofectin and lipofectamine 2000 according to the manufacturer's protocols.

Kinetic analysis of RNA synthesis with isolated nuclei

Nuclei from exponentially growing FM3A cells (1×10^8) were prepared and an RNA synthesis reaction was performed by the method of Marzluff and Huang [8]. The reaction mixtures contained 500 μM each of ATP and UTP, 50 μM [8-^{3}H]GTP, 6–18 μM CTP, and 0–40 nM ECTP, and nuclei at $2 - 5 \times 10^7$/mL. For kinetic analysis of the effect of ECTP on RNA polymerase, the initial incorporation rates of radioactivity into the acid-insoluble fraction were measured.

Immunohistochemistry

The histochemical study was performed on HT 1080 cells to observe the localization of fibrillarin in nucleolus and to explore the phosphorylation of JNK in ECyd-treated cells. After ECyd-treatment, HT 1080 cells were placed on cover glass plates. The cells were washed three times with PBS and fixed with 3% formaldehyde in PBS for 10 min. After fixation, the cells were washed twice with PBS, and were made permeable by treatment with 0.2% Triton X-100 in cold PBS for 5 min. The slides were then incubated with PBS containing 0.5% BSA as a blocking agent against non-specific surface adsorption of antibodies, for 30 min prior to treatment for 1 h with 2.5 μg/ml anti-fibrillarin antibody (Cytoskeleton, Denver, CO, USA). The same procedure was performed using 1 μg/ml anti- phosphorylated-JNK and anti-total-JNK antibodies (Cell Signaling Technology) for overnight at 4°C. The cells were then incubated with 5 μg/ml fluorescein-labeled goat anti-mouse IgG and 1 μg/ml 4′,6-diamidino-2-phenylindole dihydrochloride (DAPI) for 30 min. The cells were washed three times with PBS and covered with PermaFluor aqueous mounting medium (Invitrogen, Oregon, USA). Stained cells were observed with an Olympus BX60 microscope (Olympus, Tokyo, Japan) fitted with appropriate fluorescence filters.

Preparation of RNA and Northern blots

For the preparation of total RNA from FM3A and HT 1080 cells, QIAshredder and RNeasy kits were used (Qiagen, Hilden, Germany). RNA (2 μg/ml) was denatured in formaldehyde and then electrophoresed on a 1% agarose–formaldehyde gel. The RNA was then transferred to a Hybond-N^+ nylon membrane (Amersham, Piscataway, NJ, USA) and hybridized to ^{32}P-labeled DNA probes. The sequences of oligonucleotide probes are shown in Table 1.

Rapid amplification of 5′ cDNA ends

To identify 5′-terminal sequences of the 1.5 kb fragment formed from 28S rRNA on ECyd-treatment, 5′-RACE was performed with a kit for rapid amplification of cDNA ends (version 2.0, Invitrogen). The following oligonucleotides were used: 5′-TCAAGCTCAACAGGGTCT-3′ (antisense of nucleotides 3561–3578) for the first-strand cDNA synthesis and 5′-CGCTGGATAGTAGGTAGGGA-3′ (antisense of nucleotides 3495–3514) for the subsequent PCR. Amplified cDNA was sequenced by a sequencer (PRISM 310, ABI).

Preparation of ribosomal fractions

FM3A cells (1×10^8) were spun down, washed twice with ice-cold PBS, and resuspended in 1.5 volumes of 20 mM KCl, 5 mM Tris–HCl (pH 7.6), 1.25 mM Mg acetate, and 1.25% glycerol, and then homogenized with a Teflon-Potter homogenizer. The homogenates were centrifuged for 15 min at $16{,}000 \times g$ to remove insoluble materials. Ribosomes were obtained by centrifuging cellular lysate (0.7 ml, corresponding to 5×10^7 cells) prepared as above through a cushion of 1.3 M sucrose, 50 mM Tris–HCl (pH 7.6), 2 mM $MgCl_2$, 50 mM KCl at $190{,}000 \times g$ for 2.5 h at 4°C. The ribosomes were resuspended in 0.25 mM sucrose, 50 mM Tris–HCl (pH 7.6), 2 mM $MgCl_2$, and 50 mM KCl, and stored in aliquots at −80°C.

rRNA cleavage assay

RNase L (0.2 μg/ml) was pre-incubated in the presence of 120 nM 2-5A in 20 mM Tris–HCl (pH 7.5), 10 mM Mg acetate, 8 mM 2-mercaptoethanol, 90 mM KCl at 0°C for 30 min, prior to the addition of ribosomes (corresponding to 3 μg rRNA). The cleavage reactions were performed in a final volume of 20 μl with an incubation at 30°C. RNase A and RNase T_1 were individually incubated with ribosomes in 0.3 mM NaCl at 30°C for desired periods. These reaction mixtures were then diluted tenfold with 100 mM Tris–HCl (pH 8.0), 100 mM NaCl, 1 mM EDTA, and RNA was extracted with phenol, and the aqueous phase was re-extracted and the cleavage products were analyzed by a 2.2% agarose gel-electrophoresis.

Table 1 Northern hybridization with the specific probes for mouse and human 28S rRNA in ECyd-treated cells

	Probe sequence	Position in 28S rRNA	
		Mouse	Human
1.	5′-CCGTTACTGAGGGATCCTGGTTAGTTTCTTTTCCTCCGC-3′	52–91	52–91
2.	5′-AAAGGACGGGGGGTCTCCCCGG-3′	2,731–2,752	
3.	5′-GGGTTGGACCCGCCGCCCCGGAG-3′	2,876–2,898	
4.	5′-GAACACCGACGCGGAGGTTC-3′	3,167–3,186	
5.	5′-GCGGGCCTTCGCGATGCTTTGTT-3′	3,303–3,325	
6.	5′-ACCCAGAAGCAGGTCGTCTACGAATGGTTTAGCGCCAG-3′	4,610–4,648	4,610–4,648

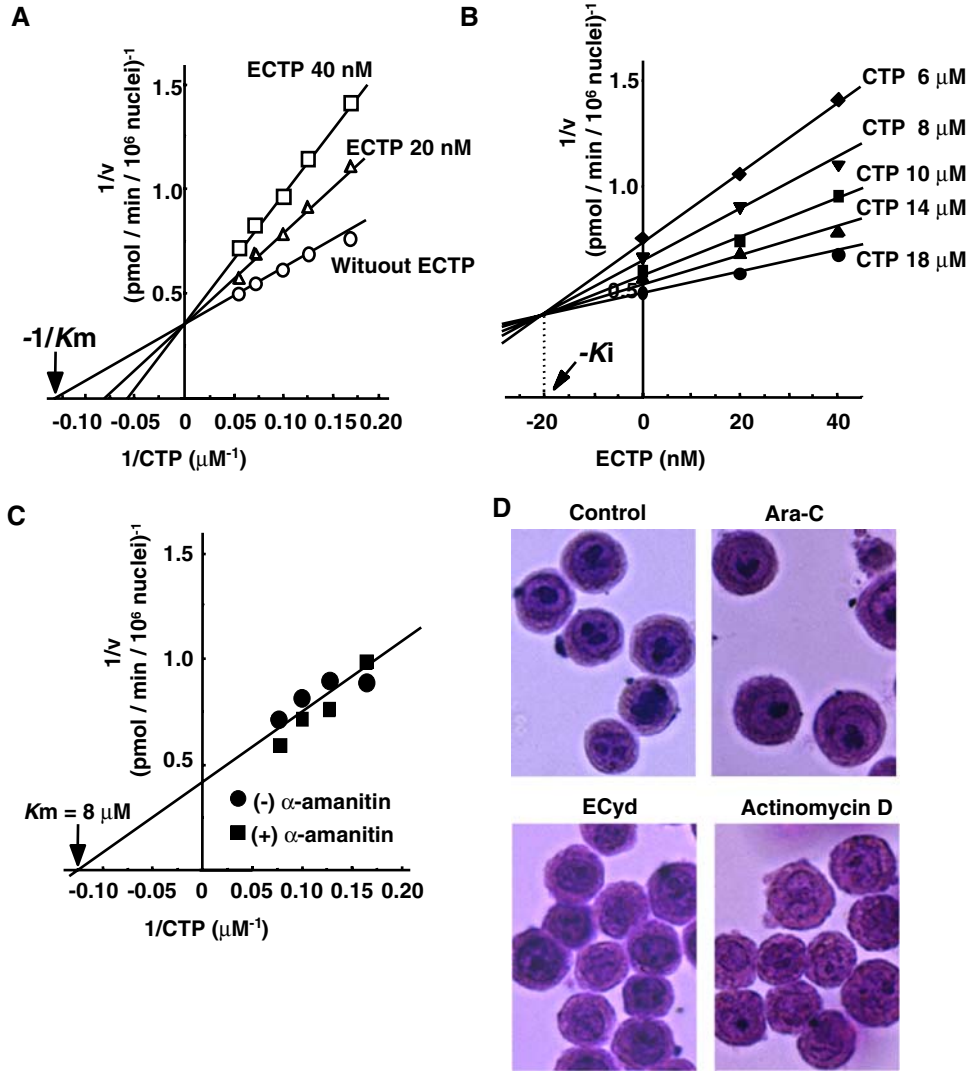

Fig. 1 Kinetic analysis of the effect of ECTP on RNA polymerase I in isolated nuclei. The K_m value for CTP and the K_i value for ECTP were determined by a Lineweaver-Burk plot (**a**) and a Dixon plot (**b**), respectively. **c** The effects of α-amanitin on RNA synthesis in isolated nuclei from FM3A cells. α-Amanitin was used at 100 μg/ml. *Points* means of triplicate analysis with ±SD of less than 5%. **d** The morphological changes in nucleoli were evaluated with Azure C staining in FM3A cells. FM3A cells were treated with either ECyd (3 μM), actinomycin D (0.21 μM) or ara-C (44 μM) for 4 h

Western blotting

HT 1080 cells were suspended in 20 mM HEPES (pH 7.5), 10 mM K acetate, 15 mM Mg acetate, 1 mM dithiothreitol, 1 mM phenylmethyl sulfonylfluoride, 10 μg/ml aprotinin, and 0.5% (v/v) Nonidet P-40, and homogenized with a tight-fitting glass Dounce homogenizer on ice. Insoluble materials were removed by centrifugation at 10,000×*g* (at 4°C for 10 min). Proteins in soluble fractions were separated on 7.5% polyacrylamide gels containing SDS and transferred to polyvinylidene difluoride membranes (Millipore, Bedford, MA, USA). For detection of phosphorylated JNK, HT 1080 cells were homogenized in Phosphosafe Extraction Buffer (Novagen, Madison, WI, USA). After cell lysis, the samples were centrifuged at 16,000×*g* for 5 min. Proteins (20 μg) were separated by 12.5% polyacrylamide gel-electrophoresis. Western blotting was done with individual antibodies. The secondary antibodies used were horseradish peroxidase-conjugated anti-mouse IgG antibody (Amersham). Immunoreactive bands were detected by enhanced chemiluminescence (Amersham) and subsequent exposure to X-ray film.

TUNEL assays

HT 1080 cells were plated onto glass coverslips precoated with poly-L-lysine. According to the TUNEL protocol (#TB235; Promega, Madison, WI, USA), cells were washed with PBS, fixed with 4% paraformaldehyde for 25 min, and rinsed three times with PBS. Cells were then permeabilized with 0.2% Triton X-100 in PBS, rinsed twice with PBS, and equilibrated with 100 μl of equilibration buffer at room temperature for 10 min. The DNA nick-labeling reaction was performed using 50 μl terminal deoxynucleotidyl transferase (TdT) incubation-buffer. The buffer contained 45 μl equilibration buffer, 5 μl nucleotide mix including fluorescein-12-dUTP (Promega, Madison, WI, USA) and 1 μl TdT for 60 min at 37°C. The reaction

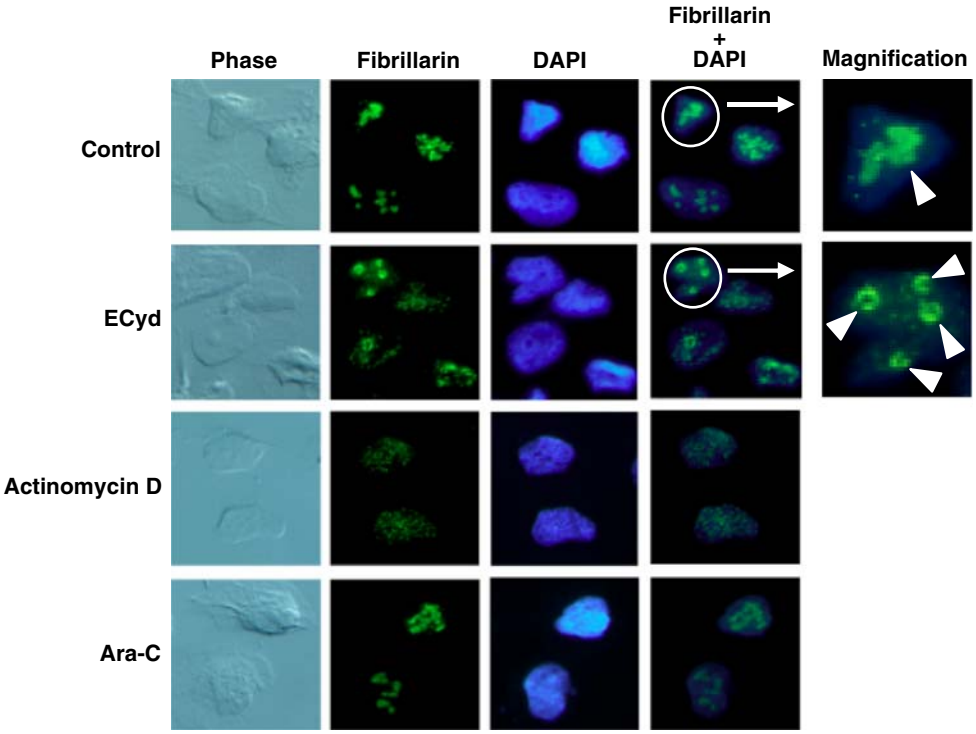

Fig. 2 Localization of fibrillarin in ECyd-treated cells. HT 1080 cells were treated with *ECyd* (1.3 μM), *actinomycin D* (25 μM) or *ara-C* (34 μ) for 4 h. Immunolocalization of *fibrillarin* (*green*) and nuclear morphology (*blue*) was visualized by confocal immunofluorescence microscopy. Nuclei were stained with *DAPI*

was then terminated by immersing the slides in 2× SSC for 15 min at room temperature. The samples were rinsed three times with PBS and mounted for analysis under a fluorescence microscope using a standard fluorescein filter, set to view through the microscope using standard fluorescein at 520 nm.

Radiolabelled RNase L substrate assay

HT 1080 cells were washed once with PBS, scraped into a minimal volume of ice-cold PBS and pelleted at 500×*g* for 5 min. Pellets were stored at −70°C until required. Pellets were then lysed in approximately twice the pellet volume of the cell lysis reagent (Sigma). After 15 min on ice, the lysate was centrifuged and the protein concentration was measured (Pierce, Rockford, IL, USA). A synthetic oligoribonucleotide $C_{11}UUC_7$ was end-labeled with [^{32}P]ATP using T4-polynucleotide kinase (Qiagen) for use as a probe. The labeled oligoribonucleotide was then purified using a spin column with twice washing with 10 mM Tris, and 1 mM EDTA (TE) and eluting with 50 μl of elution buffer. A 2.5 μg of protein in cell lysates was incubated with 2 μl of labeled probe in 20 μl of reaction mixture for 30 min at 30°C. Electrophoresis was performed on a 20% acrylamide/7 M urea/Tris–borate–EDTA (TBE) gel followed by autoradiography. Aliquots of each protein sample were subjected to Western blotting using probes for RNase L and GAPDH.

Detection of mitochondrial membrane potential

HT 1080 cells were stained with the cationic dye, 5,5′,6,6′-tetrachlorol-1′,3,3′-tetraethyl-benzimidazolylcarbocyanine iodide (JC-1; Molecular Probes) to determine the state of mitochondrial membrane potential. JC-1 is a potentiometric dye that exhibits a membrane potential-dependent loss. HT 1080 cells were incubated with RPMI1640 medium containing 10% serum and 1 μg/ml JC-1 at 37°C for 15 min. Following incubation, the cells were rinsed twice with PBS and images were obtained using a fluorescence microscope (Olympus).

Results

ECTP was a strong and competitive inhibitor of RNA polymerase I

Earlier, we found that in cells ECyd is phosphorylated to ECTP, resulting in the inhibition of RNA synthesis without changing the normal ribonucleoside triphosphate pool [3]. This finding indicated that RNA synthesis is inhibited at the RNA polymerization step. To determine the inhibitory mechanism of polymerization, we investigated the inhibition of RNA synthesis by ECTP using nuclei isolated from FM3A cells. The results obtained by a Lineweaver-Burk plot indicated that ECTP inhibits the synthesis in a competitive

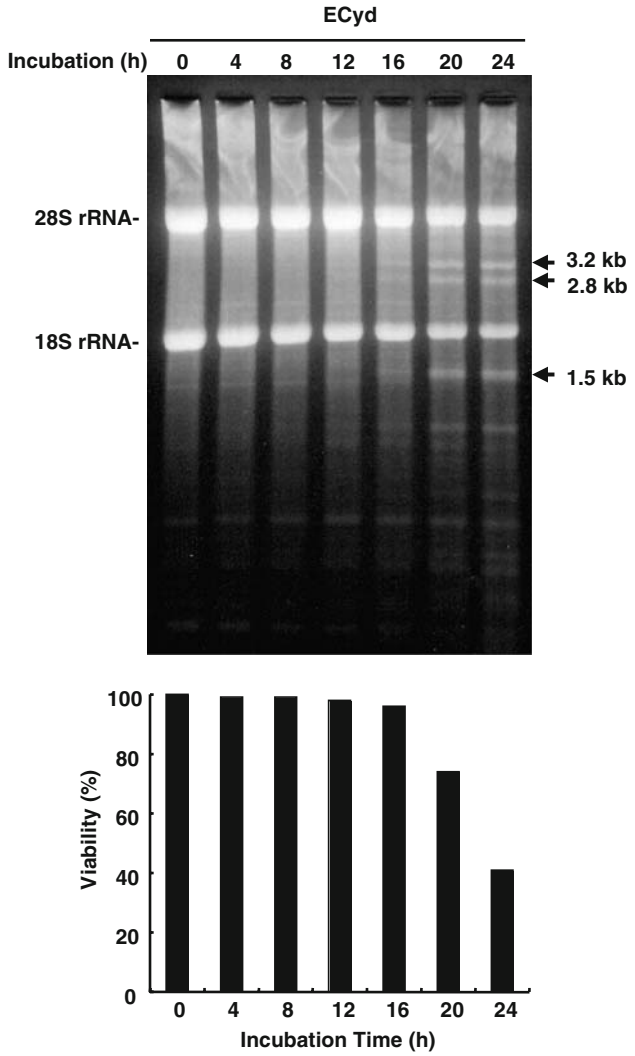

Fig. 3 28S rRNA fragmentation induced by ECyd-treatment. Total RNA was isolated at the indicated time from FM3A cells (3.7×10^5), that had been treated with ECyd (3 μM), and analyzed by 2.2% agarose gel electrophoresis. The cleavage products (3.2, 2.8 and 1.5 kb) are indicated by *arrows*. The cell viability was determined by the trypan blue staining, and the percentage of living cells was plotted on graph

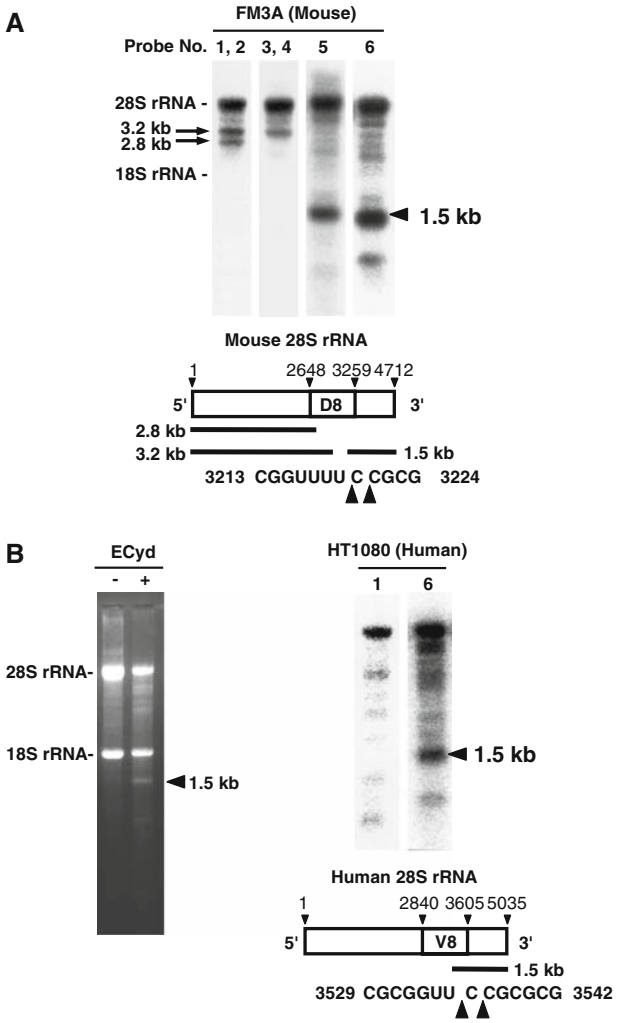

Fig. 4 Identification of rRNA fragments. **a** Northern blot analysis of fragmented rRNA. Total RNA was isolated from the FM3A cells that had been treated with ECyd (3 μM) for 24 h, electrophoresed, and subjected to Northern blotting with the labeled oligonucleotide probes as described in "Materials and methods". Fragments 3.2, 2.8 and 1.5 kb are highlighted by *arrows*. The 5′-terminal sequence of 1.5 kb was determined by 5′-RACE as described in Materials and methods". The cleavage sites are represented by *arrowheads*. nt, nucleotides. **b** *left column*: total RNA from HT 1080 cells that had been treated with ECyd (1.3 μM) for 32 h was separated by 2.2% agarose gel electrophoresis. The 1.5 kb fragment is indicated by an *arrow*. **b** *right column*: Northern blot analysis of 1.5 kb fragment, and identification of the cleavage site by 5′-RACE

manner (Fig. 1a). The apparent K_i value of ECTP for the RNA synthesis was 20 nM, as derived from the Dixon plot analysis (Fig. 1b). We used α-amanitin for positive controls in inhibiting RNA polymerase II and III. α-Amanitin at a concentration of 100 μg/ml was reported to be sufficient to inhibit both RNA polymerases II and III [9], and it showed in our hands little effect on the velocity of the RNA synthesis, may be indicating that the RNA synthesis in nuclei occurs mainly by RNA polymerase I (Fig. 1c). Nucleoli are the main intracellular location sites for RNA polymerase I, a key enzyme involved in the transcription process of pre-ribosomal RNA (pre-rRNA) during initial ribosome biogenesis. Following treatment of FM3A cells with ECyd, nucleolus shrinkage was observed within 4 h after the RNA synthesis was inhibited. These morphological changes in the nucleoli were also observed by actinomycin D, an inhibitor of RNA synthesis, but not by ara-C, an inhibitor of DNA synthesis (Fig. 1d).

ECyd induced characteristic nucleolar changes subsequent to RNA synthesis inhibition

Using human cancer cell line HT 1080, we observed the changes of nucleolus by detecting fibrillarin in ECyd-treated

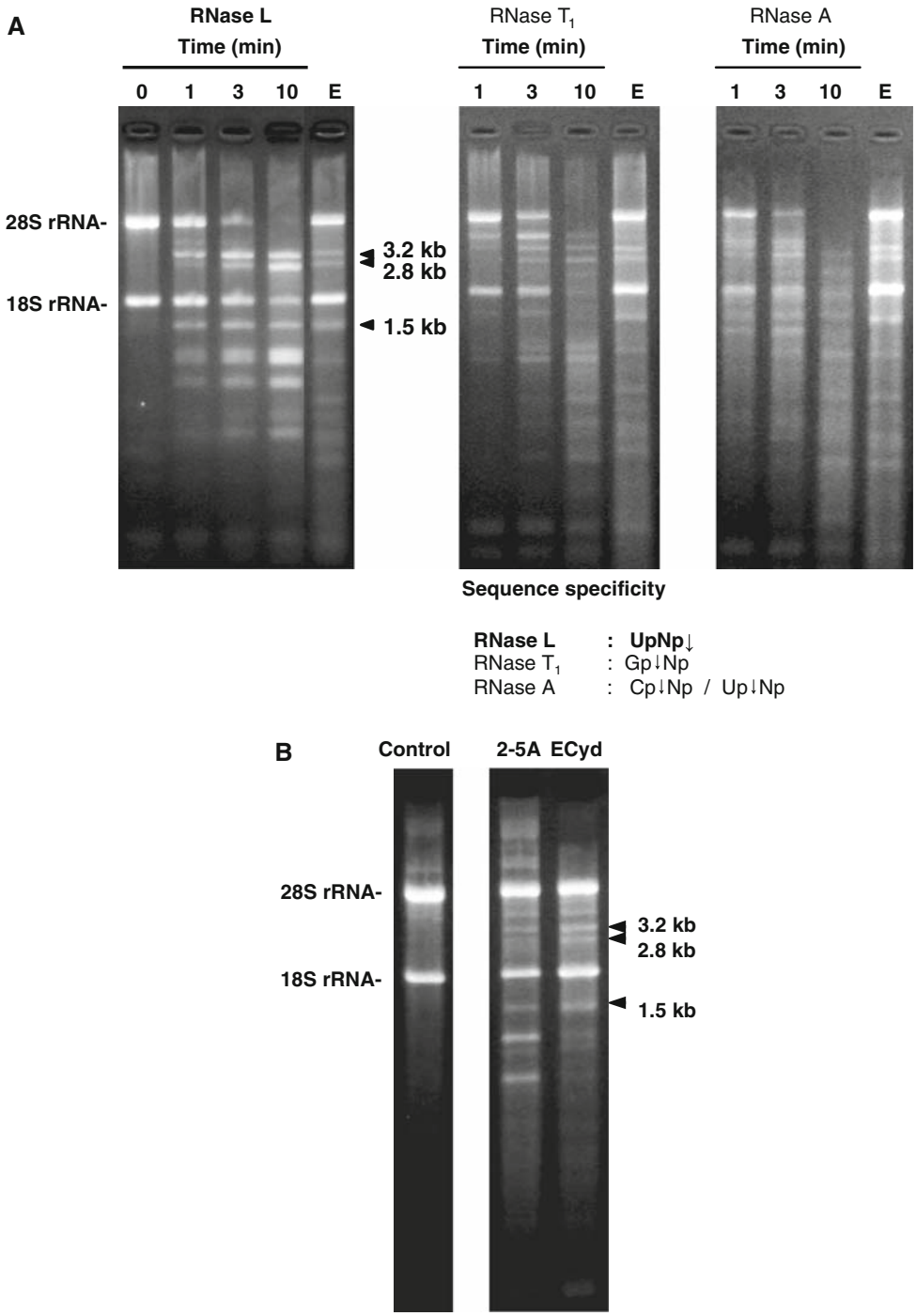

Fig. 5 The fragmentation pattern of rRNA induced by ECyd-treatment was identical to that cleaved by RNase L. *A*, Ribosomal fractions (corresponding to 3 μg RNA) prepared from FM3A cells were incubated with human RNase L (0.2 μg/ml) in the presence of 2-5A (120 nM). RNase A and RNase T_1 were incubated with ribosomes in 0.3 mM NaCl at 30°C for the indicated time. *E* ECyd-treatment induces 28S rRNA fragmentation pattern. The sequence recognized by RNase L, T1 and A are shown. **b** FM3A cells were treated with 2-5A (5 μM) in the presence of lipofectin (2 μg/ml) for 4 h according to the manufacturer's protocol (Invitrogen). The control shows cells treated with lipofectin only. The cleavage products were analyzed by 2.2% agarose gel electrophoresis

cells. Fibrillarin, a protein scatteringly located in the nucleoli, is directly involved in many post-transcriptional processes such as pre-rRNA processing, pre-rRNA methylation and ribosome assembly [10]. As shown in Fig. 2, control cells with no drug treatment showed bright clumpy nucleolar staining. Treatment with ECyd caused dislocation of fibrillarin within 4 h and formed ring-like structures, possibly involving remnant nucleoli (Fig. 2). Dispersion of fibrillarin was also induced by actinomycin D [11], but not by ara-C.

Considering that this nonhomogeneous distribution of fibrillarin was probably caused by the depletion of pre-rRNA, we monitored the amount of rRNA, a resultant product of pre-rRNA processing, in ECyd-treated FM3A cells. The amount of rRNA had decreased to 67% from the basal amount at 8 h after treatment with ECyd. Moreover, an

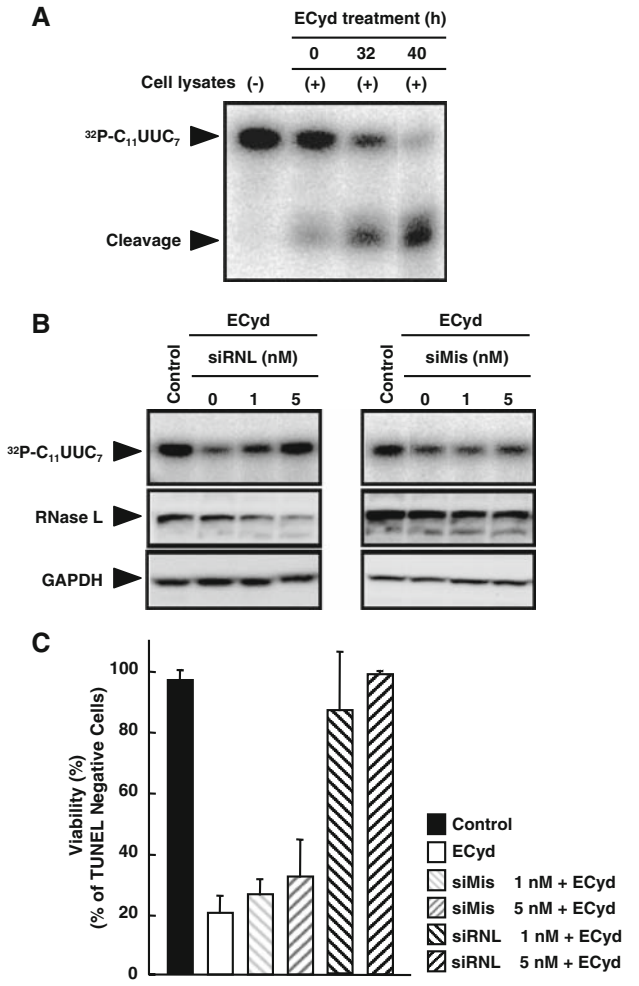

Fig. 6 RNase L activity assay demonstrating cleavage of a radiolabeled RNase L-specific substrate (5′ ^{32}P-$C_{11}UUC_7$). **a** A single-stranded RNA probe ($C_{11}UUC_7$) was end-labeled with [^{32}P]ATP and incubated with lysates prepared from ECyd-treated HT 1080 cells for indicated times. **b** RNA probe was incubated with lysates from ECyd-treated cells with siRNL or siMis. *siRNL* siRNA against RNase L. *siMis* a 4-bp mismatch introduced in RNase L siRNA. After incubation, the reaction mixtures were run on an acrylamide gel followed by autoradiography and Western blotting using antibody for RNase L and GAPDH. **c** Apoptotic cells were measured by TUNEL assays in triplicate, and ±SD were calculated

extensive fragmentation of rRNA was observed at 16 h of the treatment, accompanying a decrease in viability (Fig. 3).

rRNA fragmentation occurred in the D8 domain of 28S rRNA after treatment of cells with ECyd

In ECyd-treated FM3A cells, characteristic 3.2, 2.8, and 1.5 kb bands of RNA were formed. This was accompanied by decreases in the amounts of 28S rRNA (Fig. 3). To verify whether these fragments were derived from 28S rRNA, Northern blot analysis was performed with specific probes for various parts of 28S rRNA. Both 3.2 and 2.8 kb bands hybridized with a probe for the 5′-terminal of 28S rRNA, while a 1.5 kb band hybridized with a probe for the 3′-terminal of 28S rRNA (Fig. 4a). In contrast, the probe for 18S rRNA failed to detect any corresponding bands (data not shown). A 3.2 kb band was detected with a probe No. 4 but not with No. 5. The 2.8 kb band was detected with probe No. 2 but not with No. 3. These data indicate that 3.2 and 2.8 kb bands were the products of 28S rRNA cleavage and those sites were at somewhere from 3186 to 3303, and from 2752 to 2876, respectively (Table 1). To determine the cleavage site in mouse 28S rRNA, the 1.5 kb fragment was isolated, followed by 5′-RACE to analyze its 5′-terminal sequence. As a result, the 5′-end base of the 1.5 kb fragment was found to be nucleotide 3219 U or 3220 C (Fig. 4a). These data confirmed that the fragmented bands originated from D8 domain [12].

Similar RNA fragmentation was observed for the human cell line HT 1080 as well. Thus, as Fig. 4b shows, ECyd-treated HT 1080 gave the 1.5-kb RNA fragment in the Northern blot analysis, and the cleavage site was identified as UpNp (Np being 3535 Up or 3536 Cp). This observation suggests that the ECyd-induced apoptosis is associated with this specific rRNA-fragmentation in a ubiquitous fashion.

The ECyd-induced cleavage pattern of rRNA was similar to that induced by RNase L, and their cleavage sites were identical.

It was reported that the D8 domain of rRNA is placed on the surface of the 60S subunit, and that it could be cleaved by some RNases [12–14]. To examine whether or not 28S rRNA is cleaved by RNase L in FM3A cells treated with ECyd, the isolated ribosomal fraction from FM3A cells was subjected to hydrolysis by human recombinant RNase L. Remarkably, the RNase L-cleaved fragmentation pattern of rRNA was similar to that of ECyd-induced one (Fig. 5a). On the other hand, two other enzymes with different sequence preferences, RNase T_1 and RNase A, showed different cleavage patterns (Fig. 5a). To activate intrinsic RNase L, 2-5A transfected FM3A cells can be used. The 28S rRNA fragments of 3.2, 2.8, and 1.5 kb were indeed formed by the 2-5A treatment (Fig. 5b). In addition, the 5′-ends of the 1.5 kb fragments derived from cleavage either by recombinant RNase L or by the 2-5A transfection were identical, as determined by the RACE-assay (data not shown).

RNase L was activated, and it caused apoptosis in ECyd treated cells

To verify the RNase L activity, we measured the cleavage pattern of radiolabeled oligonucleotide, $C_{11}UUC_7$ containing a consensus RNase L cleavage site (UpNp). In fact, the oligonucleotide was cleaved on incubation with ECyd-

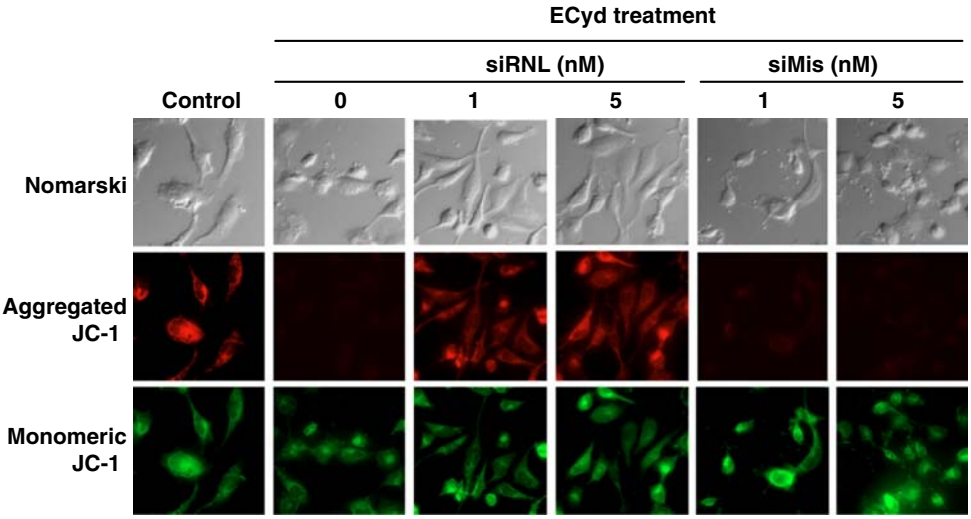

Fig. 7 The effect of RNase L-knockdown for mitochondrial membrane potential in the ECyd-treatment. HT 1080 cells were transfected with siRNL or siMis (1 or 5 nM) for 24 h prior to ECyd-treatment for 32 h (1.3 μM) and then JC-1 (molecular probes) treatment for 15 min at 37°C. *siRNL* siRNA against RNase L. *siMis* a 4-bp mismatch introduced in RNase L siRNA. In the picture "*Aggregated JC-1*", incorporation of JC-1 aggregates with *red fluorescence* into polarized mitochondria (normal mitochondria) can be seen. In contrast, in the picture "*Monomeric JC-1*", JC-1 monomers with *green fluorescence* binding to the membrane of both normal and damaged mitochondria are presented. Fluorescence microscopy analysis was performed using appropriate filters for the red fluorescence ($\lambda_{excitation}$: 546 ± 12 nm band pass filter, $\lambda_{detection}$: >590 nm long-pass filter) and the green fluorescence ($\lambda_{excitation}$: 450–490 nm band pass filter, $\lambda_{detection}$: >515 nm long-pass filter). The set of data in a given column were obtained from image-photos taken with a fixed exposure time

treated HT 1080 cell lysates in a time-dependent manner (Fig. 6a). In addition, both, the degradation of the whole oligonucleotide and the RNase L protein-expression were suppressed by treatment with an externally added siRNA against RNase L in HT 1080 cells (Fig. 6b left column). In contrast, siRNA with a 4-base mismatch sequence had no effect either for the cleavage activity or for the RNase L protein-expression (Fig. 6b right column). Also, we confirmed that the level of whole oligonucleotide was decreased on incubation with a recombinant RNase L activated by 2-5A (data not shown). As might be expected, in the RNase L-knockdown HT 1080 cells, the ECyd-induced apoptosis was suppressed (Fig. 6c). On the other hand, mismatch siRNA-treatment did not influence ECyd-induced apoptosis (Fig. 6c). In another cell line, DLD-1, a human colon cancer cell, RNase L-knockdown again suppressed ECyd-induced apoptosis (data not shown). This observation suggests that these events may be a general phenomenon for various cells.

RNase L-mediated apoptosis was dependent on mitochondrial membrane potential

A treatment of HT 1080 cells with ECyd resulted in a disappearance of red fluorescence of aggregated JC-1, indicative of dissipation of mitochondrial membrane potential (Fig. 7 middle panel). Also, the morphology of mitochondria, as detected by green fluorescence from monomeric JC-1, was disrupted in ECyd-only treated cells (Fig. 7 lower panel). On the other hand, in RNase L-knockdown HT 1080 cells, both, the levels of red fluorescence due to aggregated JC-1 and green fluorescence of JC-1 on the mitochondrial membrane were similar to those of control cells (no ECyd, no siRNA). In a mismatched siRNA-treatment, the level of red fluorescence from aggregated JC-1 was decreased, and the mitochondria showed abnormal morphology.

The JNK phosphorylation was dependent on RNase L, and led the cell to apoptosis

Figure 8a shows the level of phosphorylated JNK in ECyd-treated HT 1080 cells. The level of phosphorylated JNK increased to its maximum at 24 h of ECyd-treatment (Fig. 8a). It was notable that total JNK level (phosphorylated plus unphosphorylated) did not show any changes. When we administered anthrapyrazolone SP600125, an inhibitor of JNK action, to HT 1080 cells prior to ECyd-treatment, the apoptosis was suppressed with SP600125, in a dose dependent manner (Fig. 8b, c).

In order to analyze the effect of RNase L on the phosphorylation of JNK in HT 1080 cells, siRNA for RNase L was used to knockdown the RNase L protein expression. The level of phosphorylated JNK was decreased in the knocked-down cells, whereas the JNK-phosphorylation was maintained high in both the ECyd-only and ECyd-plus-mismatching siRNA treatments (Fig. 9). On the other hand, the fluorescence levels, that represent total JNK, were the same in all of these treatments.

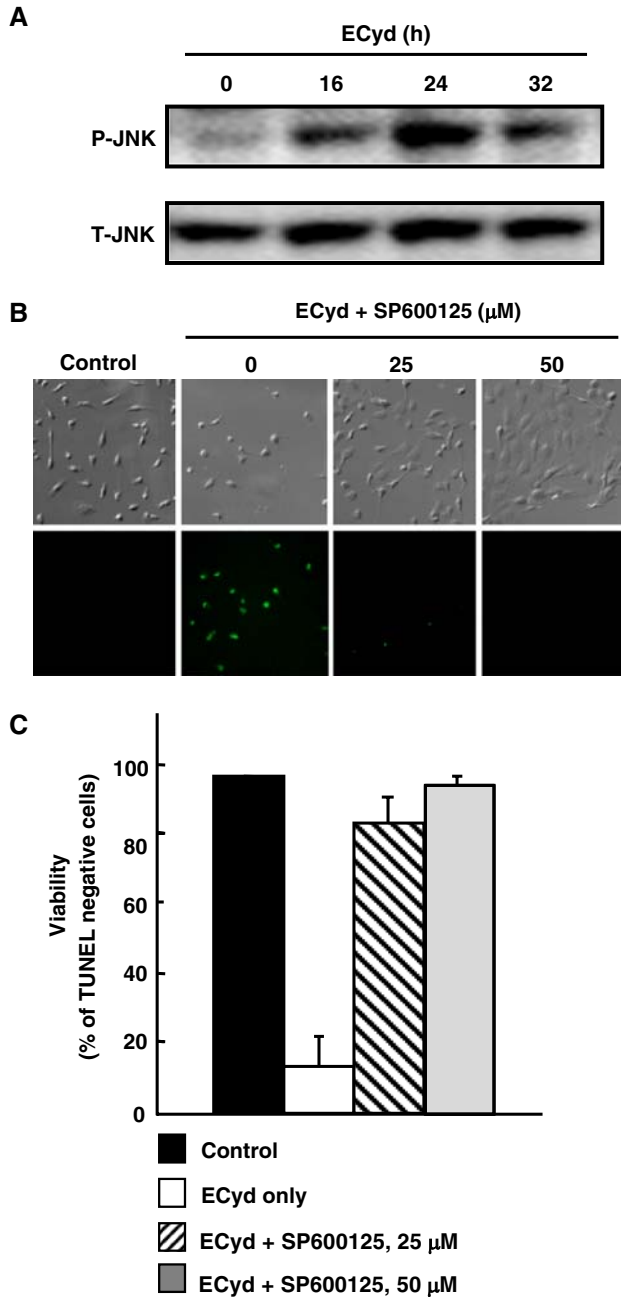

Fig. 8 The effect of JNK for ECyd-induced apoptosis. HT 1080 cells were treated with ECyd for 32 h in the absence or presence of Sp600125 (25 or 50 μM). **a** Western blots probed with antibodies to phosphorylated *JNK* (*P-JNK*) and total *JNK* (*T-JNK*) was performed at designated times of ECyd-treatment. **b** Changes in cellular morphologies. Green fluorescence represents apoptotic cells as a result of the TUNEL assay. **c** TUNEL-positive apoptotic cells were counted, and the percentage of apoptotic cells was plotted on a graph. Values are mean ± SD of triplicate samples at the indicated times

Figure 10 shows the change of mitochondrial membrane potential by treatment with JNK inhibitor, SP600125 in HT 1080 cells. As shown in the Figure, the mitochondrial membrane potential was resumed by the use of JNK inhibitor (Fig. 10 middle and lower panels). In contrast, ECyd-only treatment resulted in a null mitochondrial membrane potential.

Discussion

In this work, we show that ECyd induces nucleolar alterations and 28S rRNA fragmentation following the inhibition of RNA synthesis (Figs. 1, 2, 3). Actinomycin D, a known RNA synthesis inhibitor, also induces the change of nucleolar morphology. The interesting possibility that actinomycin D may induce similar RNA fragmentation in the cells is currently being explored. It should be noted that α-amanitin, an inhibitor to RNA polymerase-II and -III but not to RNA polymerase I [9], did not influence the velocity of RNA synthesis (Fig. 1c). These results suggest that ECyd induces inhibition of RNA polymerase I-activity. These disruptions in RNA status might represent a trigger mechanism for the apoptotic signaling pathway. Our results suggest that RNase L plays an important role for 28S rRNA fragmentation and for apoptosis induced by ECyd-treatment (Figs. 4, 5, 6). We show that RNase L mediates the apoptosis and the loss of mitochondrial membrane potential induced by ECyd treatment (Fig. 7). These suggest that the inhibition of RNA synthesis leads to mitochondria-dependent apoptosis, and that RNase L is required for this apoptosis. RNase L is a unique enzyme requiring $p(A2'p)_nA$ (2-5A), an unusual oligoadenylates with 2′–5′ phosphodiester linkages. 2-5A is produced from ATP by a family of 2′–5′ oligoadenylate synthetases (OAS) and binds to monomeric inactive RNase L to form a homodimeric active enzyme [15]. Previously, it was reported that the role of RNase L was to eliminate RNA-viruses in infected cells and to regulate the cell cycle, cell growth, and RNA metabolism with its endonucleolytic activity [16]. Our present study suggests that RNase L can potentiate the cellular suicidal pathway.

The inhibition of RNA synthesis has been shown by Morten et al. [17] to induce a morphological change in the nucleolus together with an alteration of nucleolar protein localization, prior to eventual apoptosis. Furthermore, RNA polymerase I is known to localize in the nucleolus where it transcribes rDNA to generate precursor transcripts of mature rRNA species. ECyd-treatment induced a morphological change of nucleoli in the nucleolus (Fig. 2), a phenomenon with which we hypothesize that the activity of RNA polymerase I might be inhibited in ECyd-treated cells. Our data also demonstrated that the events after the inhibition of RNA synthesis proceed via 2-5A/RNase L-activated pathway. Thus, RNase L is activated after nucleolar changes as a result of RNA synthesis inhibition (Fig. 6). Therefore, the RNase L-activating factor(s) may be produced under conditions of transcriptional inhibition. OAS requires ATP to produce the 2-5A, thereby RNase L is

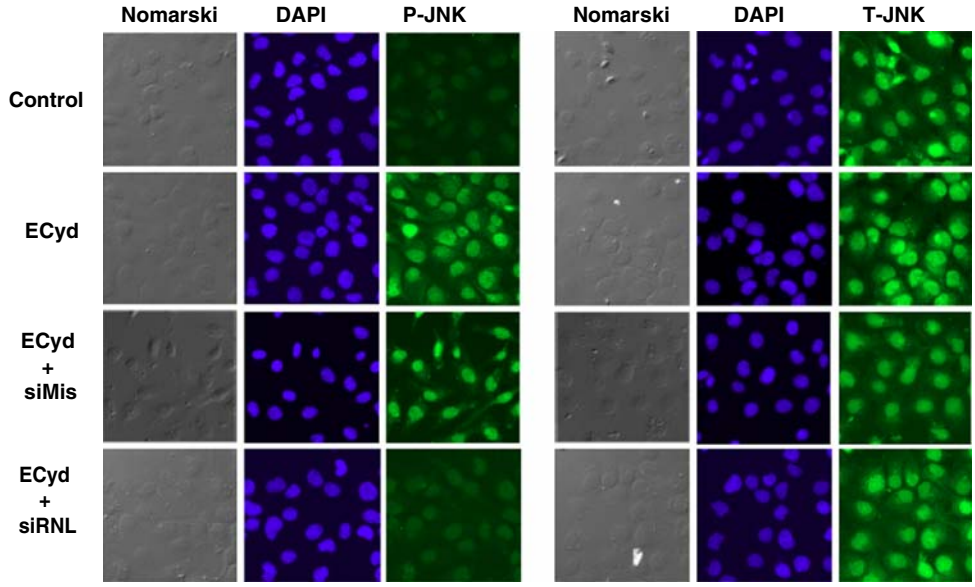

Fig. 9 The phosphorylation of JNK by RNase L. HT 1080 cells were transfected with siRNL and siMis 24 h prior to ECyd-treatment for 24 h. *siRNL* siRNA against RNase L. *siMis* a 4-bp mismatch introduced in RNase L siRNA. Phosphorylated JNK (*P-JNK*) and total JNK (*T-JNK*) were detected by immunofluorescence (IF) with specific antibody (Cell Signaling Technology). Nuclei were stained with *DAPI*. *Green fluorescence* represents IF: *P-JNK* and *T-JNK*. Control indicates lipofectamine-only treated cells. The set of data in a given column were obtained from image-photos taken with a fixed exposure time

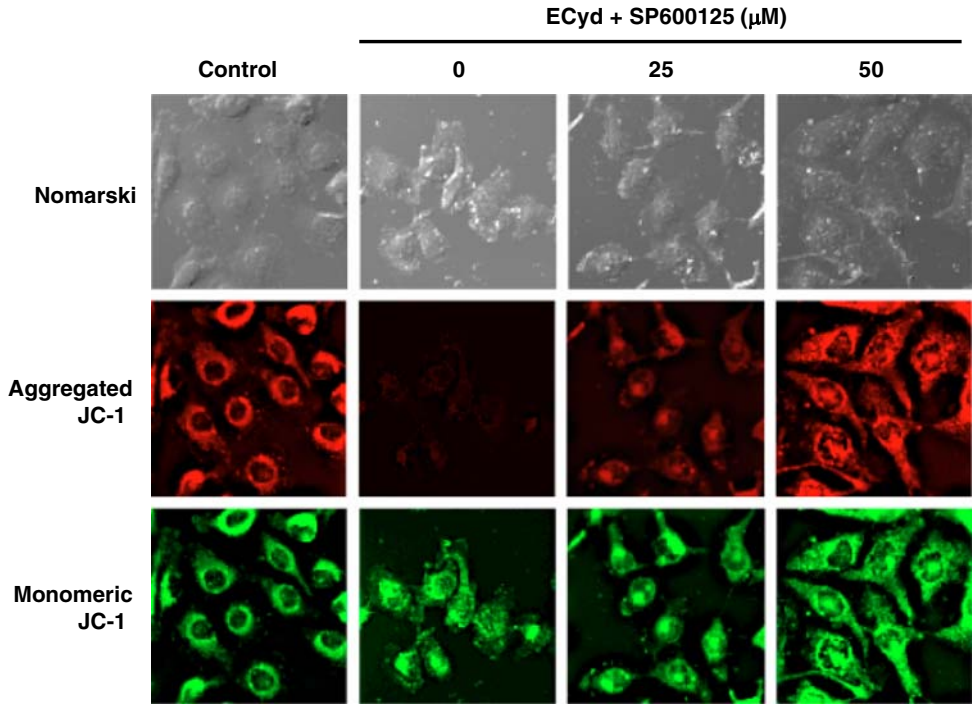

Fig. 10 The change of mitochondrial membarane potential by JNK phosphorylation. HT 1080 cells were treated with ECyd for 32 h in the absence or presence of JNK inhibitor Sp600125 (25 or 50 μM) and then were treated with JC-1 (Molecular Probes) for 15 min at 37°C. Mitochondrial depolarization was detected by using JC-1. In the picture "*Aggregated JC-1*", incorporation of JC-1 aggregates with *red fluorescence* into polarized mitochondria (normal mitochondria) can be seen. In contrast, in the picture "*Monomeric JC-1*", JC-1 monomers with *green fluorescence* bind to the membrane of both normal and damaged mitochondria are shown. Fluorescence microscopy analysis was performed using appropriate filters for the red fluorescence ($\lambda_{excitation}$: 546 ± 12 nm band pass filter, $\lambda_{detection}$: >590 nm long-pass filter) and the green fluorescence ($\lambda_{excitation}$: 450–490 nm band pass filter, $\lambda_{detection}$: >515 nm long- pass filter). The set of data in a given column were obtained from image-photos taken with a fixed exposure time

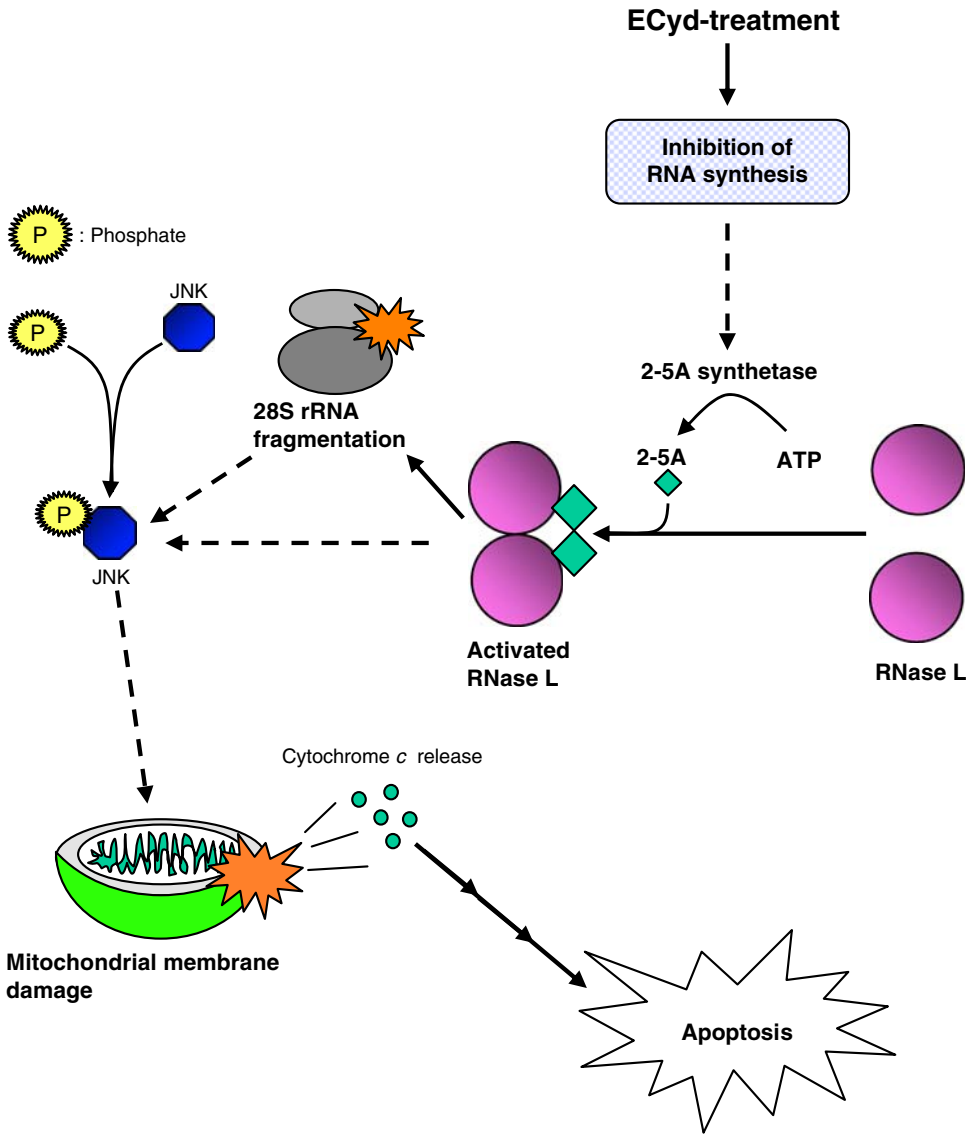

Fig. 11 Scheme of apoptotic signal pathway mediated by RNase L in ECyd-treated cells

activated. We have also reported that the intracellular concentration of ATP increased as a consequence of transcriptional inhibition in ECyd-treated FM3A cells [1]. Such ATP-rich environment would promote the OAS-mediated production of 2-5A. It was reported that OAS can be activated by RNA aptamers as well, in addition to activation by dsRNA [18]. Another report suggested that RNase L activation is associated with removal of abnormal cellular RNAs [19]. Thus, immature RNAs may possibly be produced in our experimental settings; thereby RNase L activation might become necessary to remove such abnormal RNAs in the cells. Although it is reported that a type of disruption of nucleolus structure can induce apoptosis, mechanisms involved in it is unknown [20].

It has been documented that activation of RNase L leads to activation of c-Jun N-terminal kinase (JNK), followed by mitochondrial release of cytochrome *c* and subsequent caspase-dependent apoptosis [21–23]. In our study, RNase L was activated and mitochondrial membrane potential was decreased in ECyd-treated cells. Therefore, it is expected that JNK phosphorylation may occur in the RNase L-dependent apoptotic signal pathway induced by ECyd. We investigated the phosphorylation of JNK in ECyd-treated HT 1080 cells. Indeed, JNK was found to be phosphorylated in these cells, and, moreover, a JNK inhibitor, SP600125, suppressed the apoptosis (Fig. 8). These data indicate that the ECyd-induced apoptosis is regulated by JNK signaling. The results shown in Figs. 9 and 10 support the notion that RNase L induces apoptosis through the phosphorylation of JNK. Thus, the apoptotic pathway may be summarily drawn as shown in Fig. 11. In addition, we have obtained data that suggest some aspects of downstream events: i.e., caspases -9 and -3 seem to be activated, subsequent to a release of cytochrome c from mitochondria,

and then induction of DNA-fragmentations and apoptosis-like morphological changes follow (to be published elsewhere). However, it is not clear how activated RNase L leads to JNK phosphorylation. Once this new function of RNase L has been elucidated, novel targets for antitumor agents might emerge.

Recent literature shows that antibiotics (anisomycin, blasticidin S), ultraviolet-C, B, and α-sarcin can cause cleavage of cellular 28S rRNA, accompanying JNK phosphorylation. Thus, 28S rRNA cleavage seems to be associated with JNK phosphorylation [24–26]. Figures 3, 4 and 5 show that RNase L cleaves 28S rRNA in ECyd treated cells. These RNA fragments may act as mediator of the activation of JNK. Furthermore, other researchers proposed that activated RNase L not only cleaves RNA but also can interact with other proteins (RNase L-unknown protein(s) complex) through its C-terminal domain [27–29]. Such proteins associated with RNase L may be expected to be activated, and subsequently act for the phosphorylation of JNK.

In conclusion, our findings imply that RNase L is an essential member of apoptosis, triggered by impairment of RNA synthesis. RNase L-mediated apoptosis seems to be a pathway dependent on mitochondria. Understanding of this pathway further is expected to reveal a line of drug targets in the apoptotic mechanisms.

Acknowledgments The authors thank Dr. Hikoya Hayatsu (Faculty of Pharmaceutical Sciences, Okayama University) for helpful discussions. This research was partially supported by a grant for Exploractory Research (18659029, Y.W.) from the Ministry of Education, Culture, Sports, Science and Technology of Japan.

References

1. Shimamoto Y, Fujioka A, Kazuno H et al (2001) Antitumor activity and pharmacokinetics of TAS-106, 1-(3-*C*-ethynyl-*β*-D-*ribo*-pentofuranosyl) cytosine. Jpn J Cancer Res 92:343–351
2. Hattori H, Tanaka M, Fukushima M et al (1996) 1-(3-*C*-ethynyl-*β*-D-*ribo*-pentofuranosyl)-cytosine, 1-(3-*C*-ethynyl-*β*-D-*ribo*-pentofuranosyl)-uracil, and their nucleobase analogues as new potential multifunctional antitumor nucleosides with a broad spectrum of activity. J Med Chem 39:5005–5011
3. Takatori S, Kanda H, Takenaka K et al (1999) Antitumor mechanisms and metabolism of the novel antitumor nucleoside analogues, 1-(3-*C*-ethynyl-*β*-D-*ribo*-pentofuranosyl) cytosine and 1-(3-*C*-ethynyl-*β*-D-*ribo*-pentofuranosyl) uracil. Cancer Chemother Pharmacol 44:97–104
4. Takatori S, Tsutsumi S, Hidaka M et al (1998) The characterization of cell death induced by 1-(3-*C*-ethynyl-*β*-D-*ribo*-pentofuranosyl)-cytosine (ECyd) in FM3A cells. Nucleosides Nucleotides 17:1309–1317
5. Yoshimura A, Nakanishi M, Yatome C et al (2002) Comparative study on the biological properties of 2′, 5′-oligoadenylate derivatives with purified human RNase L expressed in *E. Coli*. J Biochem 132:643–648
6. Lesiak K, Torrence PF (1986) Synthesis and biological activities of oligo(8-bromoadenylates) as analogues of 5′-*O*-triphospho adenylyl(2′–5′)adenylyl (2′–5′) adenosine. J Med Chem 29:1015–1022
7. Ueno Y, Naito T, Kawada K et al (2005) Synthesis of novel siRNAs having thymidine dimers consisting of a carbamate or a urea linkage at their 3′ overhang regions and their ability to suppress human RNase L protein expression. Biochem Biophys Res Commun 330:1168–1175
8. Marzluff WF, Huang RCC (1984) Transcription of RNA in isolated nuclei Transcription and translation. IRL Press, Oxford (UK), pp 89–129
9. Chambon P (1975) Eukaryotic nuclear RNA polymerases. Annu Rev Biochem 44:613–638
10. Narcisi EM, Glover CV, Fechheimer M (1998) Fibrillarin, a conserved pre-ribosomal RNA processing protein of Giardia. J Eukaryot Microbiol 45:105–111
11. Chen M, Jiang P (2004) Altered subcellular distribution of nucleolar protein fibrillarin by actinomycin D in HEp-2 cells. Acta Pharmacol Sin 25:902–906
12. Michot B, Hassouna N, Bachellerie JP (1984) Secondary structure of mouse 28S rRNA and general model for the folding of the large rRNA in eukaryotes. Nucleic Acids Res 12:4259–4279
13. Han H, Schpartz A, Pellegrini M et al (1994) Mapping RNA regions in eukaryotic ribosomes that are accessible to methidium-propyl- EDTA.Fe(II) and EDTA.Fe(II). Biochemistry 33:9831–9844
14. Holmberg L, Melander Y, Nygard O (1994) Probing the conformational changes in 5.8S, 18S and 28S rRNA upon association of derived subunits into complete 80S ribosomes. Nucleic Acids Res 22:2776–2783
15. Dong B, Silverman RH (1995) 2–5A-dependent RNase molecules dimerize during activation by 2–5A. J Biol Chem 270:4133–4137
16. Stark GR, Kerr IM, Williams BR et al (1998) How cells respond to interferons. Annu Rev Biochem 67:227–264
17. Morten O, Christensen MO, Rene M et al (2004) Distinct effects of topoisomerase I and RNA polymerase I inhibitors suggest a dual mechanism of nucleolar/nucleoplasmic partitioning of topoisomerase I. J Biol Chem 279:21873–21882
18. Hartmann R, Nørby PL, Martensen PM et al (1998) Activation of 2′–5′ oligoadenylate synthetase by single-stranded and double-stranded RNA aptamers. J Biol Chem 273:3236–3246
19. Player MR, Torrence PF (1998) The 2–5A system: modulation of viral and cellular processes through acceleration of RNA degradation. Pharmacol Ther 78:55–113
20. Ugrinova I, Monier K, Ivaldi C et al (2007) Inactivation of nucleolin leads to nucleolar disruption, cell cycle arrest and defects in centrosome duplication. BMC Mol Biol 8:66
21. Iordanov MS, Paranjape JM, Zhou A et al (2000) Activation of p38 mitogen-activated protein kinase and c-Jun NH(2)-terminal kinase by double-stranded RNA and encephalomyocarditis virus: involvement of RNase L, protein kinase R, and alternative pathways. Mol Cell Biol 20:617–627
22. Malathi K, Paranjape JM, Ganapathi R et al (2004) HPC1/RNASEL mediates apoptosis of prostate cancer cells treated with 2′, 5′-oligoadenylates, topoisomerase I inhibitors, and tumor necrosis factor-related apoptosis-inducing ligand. Cancer Res 64:9144–9151
23. Li G, Xiang Y, Sabapathy K et al (2004) An apoptotic signaling pathway in the interferon antiviral response mediated by RNase L and c-Jun NH2-terminal kinase. J Biol Chem 279:1123–1131
24. Barr RK, Bogoyevitch MA (2001) The c-Jun N-terminal protein kinase family of mitogen-activated protein kinases (JNK MAPKs). Int J Biochem Cell Biol 33:1047–1063
25. Iordanov MS, Pribnow D, Magun JL et al (1997) Ribotoxic stress response: activation of the stress-activated protein kinase JNK1 by inhibitors of the peptidyl transferase reaction and by sequence-specific RNA damage to the α-sarcin/ricin loop in the 28S rRNA. Mol Cell Biol 17:3373–3381

26. Xia S, Li Y, Rosen EM et al (2007) Ribotoxic stress sensitizes glioblastoma cells to death receptor induced apoptosis: requirements for c-jun NH2-terminal kinase and Bim. Mol Cancer Res 5:783–792
27. Bettoun DJ, Scafonas A, Rutledge SJ et al (2005) Interaction between the androgen receptor and RNase L mediates a cross-talk between the interferon and androgen signaling pathways. J Biol Chem 280:38898–38901
28. Le RF, Salehzada T, Bisbal C et al (2005) A newly discovered function for RNase L in regulating translation termination. Nat Struct Mol Biol 12:505–512
29. Malathi K, Paranjape JM, Bulanova E et al (2005) A transcriptional signaling pathway in the IFN system mediated by 2′–5′-oligoadenylate activation of RNase L. Proc Natl Acad Sci USA 102:14533–14538